Modeling decoherence in a driven two-level system using random matrix theory

Jin Wang

Physics, Department of Natural Sciences, The University of Michigan, Dearborn, Michigan 48128, USA (jinwang@umd.umich.edu)

Received August 9, 2011; revised September 16, 2011; accepted October 19, 2011; posted October 20, 2011 (Doc. ID 152624); published December 9, 2011

Random matrix theory is used to model a two-level quantum system driven by a laser and coupled to a reservoir with N degrees of freedom in both Markovian and non-Markovian regimes. Decoherence is naturally included in this model. The effect of reservoir dimension and coupling strength between the system and reservoir is explored.

OCIS codes: 270.2500, 000.5490.

1. INTRODUCTION

The modeling of quantum systems as they interact with the reservoir is important to the fields of quantum information and computing. One important phenomenon to model is decoherence [1,2]. Decoherence occurs when a quantum system's information is dissipated into its reservoir. To describe decoherence, the master equation model of quantum systems uses the Lindblad superoperator [3–6] in order to phenomenologically add the decay parameters. The reduced density matrix ρ_s of the master equation is solved by converting it into a set of optical Bloch equations.

The random matrix theory (RMT) described in this article was originally used to successfully model the complex dynamics of spectral fluctuations of quantum systems [7]. The theory was then adapted for use in a number of areas, from chemical physics to quantum systems [8–11]. Recently the ability of the RMT combined with the Schrödinger wave function to solve a quantum system weakly coupled to its reservoir (Markovian) has been demonstrated [10]. Two new features that are investigated in this paper are varying the coupling strength between the system and the environment from weak (Markovian) to strong (non-Markovian), and study the effect of varying the reservoir dimension N on the decoherence rate.

This article is organized as follows. In Section 2, a model of a two-level quantum system coupled to a random reservoir with dimension size N is solved using the Schrödinger wave function approach. Decoherence is obtained using a partial trace over the reservoir. In Section 3, the reservoir dimension size N and coupling strength E_{sr} are varied to show their effects on the magnitude and rise time of the steady-state coherence. The effect of reservoir dimension N and the number of simulations M averaged together is discussed. A discussion of how non-Markovian behavior can be modeled using the master equation [4] is given in the concluding section.

2. THE MODEL

The RMT can simulate quantum systems with multiple energy levels interacting with a random reservoir. In this article, an example of a two-level system driven by a coherent source will be investigated. The system consists of a ground state $|g\rangle$ and excited state $|e\rangle$ coupled to a monochromatic laser field and a random reservoir with finite dimension N set by cavity parameters.

The full Hamiltonian is given by

$$H = H_s \otimes I_r + I_s \otimes H_r + H_I, \tag{1}$$

where H_s corresponds to the atom-laser coupling and is defined as

$$H_s = E_\Omega(|e\rangle\langle g| + |g\rangle\langle e|). \tag{2}$$

E_Ω represents the Rabi frequency that characterizes the coupling between the atomic dipole and the laser field. The terms I_r and I_s represent the unit operators in the Hilbert space of the reservoir and the system, respectively. The reservoir Hamiltonian is given by

$$H_r = E_r \times R. \tag{3}$$

The term H_I is the Hamiltonian describing the system–reservoir interaction, which is given by

$$H_I = E_{sr}(H_e \otimes |e\rangle\langle g| + H_g \otimes |g\rangle\langle e|). \tag{4}$$

The coefficients E_r and E_{sr} in Eqs. (3) and (4) represent the strength of the reservoir and interaction Hamiltonians, respectively.

The elements of the matrix R are chosen such that the matrix is a Gaussian unitary ensemble (GUE) with associated invariance properties [10]. The GUE was chosen over the Gaussian orthogonal ensemble due to the reservoir having complex states as will be defined later. Practically, the real and imaginary parts of each element in the Hermitian matrix R is chosen using complex Gaussian random numbers with variance 0.083 and mean of zero. This variance corresponds to the variance of a uniform distribution on the interval of −0.5 to 0.5. The Hamiltonian R is determined at the beginning and held fixed over the time evolution of each single trajectory. The matrix H_e is constructed using Gaussian random numbers

of variance 0.083 and mean of zero where each element has a real and imaginary part. The matrix H_g is created by taking the Hermitian conjugate of H_e, i.e., $H_g = H_e^\dagger$. This ensures that the interaction Hamiltonian H_I is a Hermitian matrix. The idea behind the form of interaction Hamiltonian is to set up different correlations between the system and the reservoir depending on whether the system is transitioning from the excited to ground state and visa versa. The square matrices H_r, H_e, and H_g have dimension N. These transition operators are defined as the lowering $|e\rangle\langle g|$ and raising $|g\rangle\langle e|$ operators, respectively, in Eq. (4).

The initial combined state of the system and reservoir $|\psi_0\rangle$ is a product of the pure states of the two-level system $|\psi_{s0}\rangle$ and the random reservoir states $|\psi_{r0}\rangle$:

$$|\psi_0\rangle = |\psi_{s0}\rangle \bigotimes |\psi_{r0}\rangle. \tag{5}$$

By keeping track of the reservoir state the system evolution is dependent on its history, thus allowing non-Markovian systems to be simulated. The initial random state of the reservoir $|\psi_{r0}\rangle$ is created using Gaussian complex random numbers with variance 0.083 and mean zero. The initial state of the system $|\psi_{s0}\rangle$ is the excited state $|e\rangle$, but it can take on any superposition of ground and excited states.

The wave function of the combined system and reservoir state $|\psi_t\rangle$ is found using unitary time evolution, and a partial trace to remove the reservoir states yielding the decoherence of the two-level system [12].

The standard master equation of a two-level atom driven by a laser interacting with a reservoir is given by the following:

$$\dot{\rho} = -i[H,\rho] + \gamma\mathcal{D}[|e\rangle(\langle g|]. \tag{6}$$

Here, H is the atom–laser interaction Hamiltonian and the γ is the decay rate. The decoherence due to the interaction with the reservoir is given by the Lindblad form [3]. The Lindblad superoperator $\mathcal{D}$ for arbitrary operators A and B is defined as $\mathcal{D}[A]B \equiv ABA^\dagger - \frac{1}{2}\{A^\dagger A, B\}$.

3. DECOHERENCE IN BOTH MARKOVIAN AND NON-MARKOVIAN REGIONS

The amplitude of the Rabi oscillation is set to be $E_\Omega = 1$ in this article. In Fig. 1 the coupling strength is $E_{sr} = 0.15$, which represents weak coupling between the system and the reservoir. The coupling is classified as weak or strong with respect to the strength of the driving field E_Ω. This corresponds to a Markovian process. The reservoir dimension is $N = 12$. The decoherence analysis here is based on the ensemble average evolution of 30 individual simulations of the system coupled with the reservoir. By averaging over 30 time evolutions the standard deviation has 5% error relative to the steady-state value. In each of the 30 simulations the Hamiltonian and the reservoir state are generated as random matrices and fixed for the simulation time. The decoherence is measured using the excited-state population decay rate, the system entropy S, and the ratio between the system's large and small eigenvalues.

One advantage of the RMT can be seen in the plot of the system excited-state population ρ_{ee} in the bottom of Fig. 1. Specifically, the decoherence of the system occurs naturally without the need for adding decoherence phenomenologically

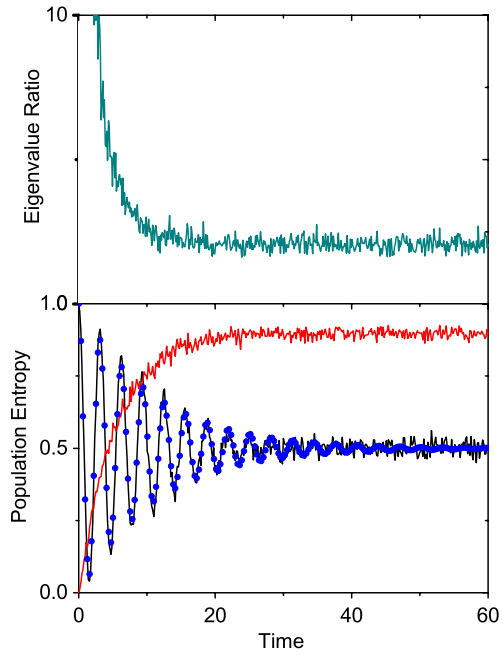

Fig. 1. (Color online) Plot of the excited-state population versus time from the random matrix model (the oscillatory line with randomness) is on the bottom plot of the figure. The dots that overlap the oscillatory line represent the excited-state population versus time as found using the master equation approach. The plot of the system entropy is shown on the bottom plot as a line starting at zero, and increasing to a steady-state value of 0.9. The top plot shows the ratio between the system large and small eigenvalues versus time in units of $1/\gamma$ starting at ∞ and decaying to 0.7. The parameters for all the plots are $E_\Omega = 1$, $E_r = 1$, $E_{sr} = 0.15$, $N = 12$. All of the plot lines are an average of the results of 30 simulations.

as is the case for the master equation approach. Assuming the damping of the system modeled using RMT is of the form $e^{-3\gamma t/4}$ [13], the decoherence rate γ is found to be 0.06160 through curve fitting. Using this decoherence rate in the master equation yields a close match to the random matrix approach. The difference is that the random matrix approach contains small random fluctuations due to the randomness in the reservoir Hamiltonian. The χ^2 measure of the curve fit between the solutions is 0.00051.

Decoherence can also be measured using the system entropy. The entropy of the reduced density matrix ρ_s of the system is found with $S \equiv -tr[\rho_s(\log_2(\rho_s))]$. The entropy curve in the bottom of Fig. 1 starts at 0 and rises to a steady-state value. This indicates that the system starts from an initially pure state with zero entropy, and then becomes a more mixed state with a steady-state entropy of around 0.9 during a time scale of a few γ^{-1}.

In addition, decoherence can be measured inversely using the ratio between the large and small eigenvalues of the reduced density of the system, as shown in the top half of Fig. 1. Since the system has only two eigenvalues, the minimum value with this measure is 1 and corresponds to a completely mixed state. The maximum value of ∞ corresponds to a completely pure state. The time evolution of the ratio between the system large and small eigenvalues yields the Schmidt path, which gives an alternative way to measure the decoherence of the system state over time.

One parameter that controls the decoherence rate of the quantum system is the reservoir dimension N. In the case

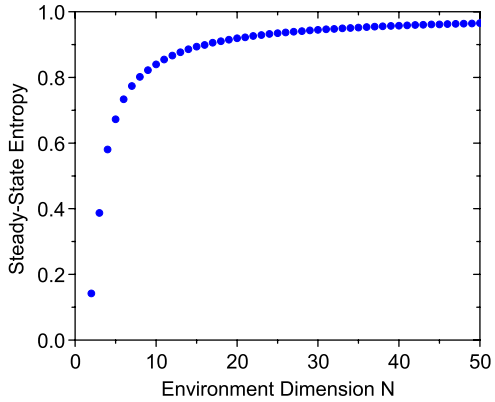

Fig. 2. (Color online) Plot of steady-state system entropy versus reservoir dimension size N. The parameters are $E_\Omega = 1$, $E_r = 1$, $E_{sr} = 0.15$.

of the master equation this corresponds to the number of harmonic oscillators, in the case of the random matrix model this corresponds to the number of elements in the reservoir model. The steady-state entropy of a system coupled to a reservoir of dimension N from 2 to 50 is shown in Fig. 2. The system will decohere faster and reach a more mixed steady-state as the dimension N increases. Also, the time required to reach the steady state decreases as the reservoir dimension N increases, as indicated in Fig. 3.

The decoherence behavior of the system also depends on the system-reservoir coupling strength E_{sr}. Up to this point weak coupling ($E_{sr}/E_\Omega = 0.15$) has been assumed. This causes the system to evolve under Markovian dynamics, and is well modeled by the master equation. Now the coupling strength is increased in order to move the system dynamics into the non-Markovian region. As shown in Fig. 4, as the coupling strength E_{sr} is increased, the system exhibits nonexponential decay behavior, which is an indication of non-Markovian dynamics [14–17] . In the extreme case when $E_{sr}/E_\Omega = 50$, the initial excited system state is frozen. This applies to any other initial system states, and is an example of the quantum zenolike effect [18–20]. The reason the method can model non-Markovian systems comes from the ability of the reservoir to store information that evolves over time while dynamically interacting with the quantum system.

Finally, the number of simulated time evolutions averaged together in the above figures is chosen to be 30. By averaging

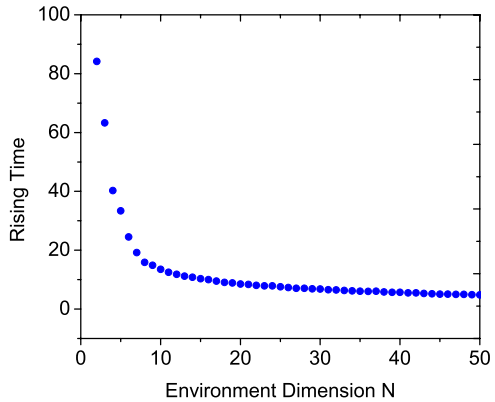

Fig. 3. (Color online) Plot of the time in units of $1/\gamma$ needed to reach 90% of the steady-state value of the entropy versus dimension N of the reservoir. The parameters used in the plot are $E_\Omega = 1$, $E_r = 1$, and $E_{sr} = 0.15$.

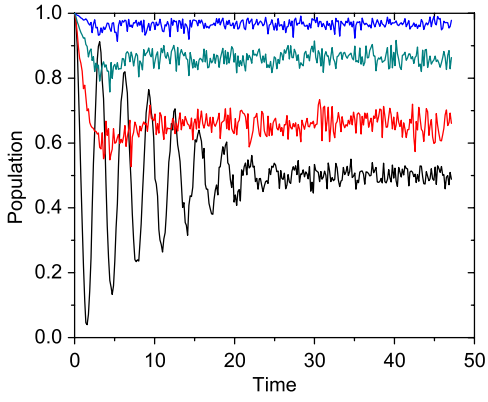

Fig. 4. (Color online) Plot of the excited-state population versus time in units of $1/\gamma$ for different coupling strengths. From bottom to top, the coupling strengths are $E_{sr} = 0.15$, 10, 30, 50.

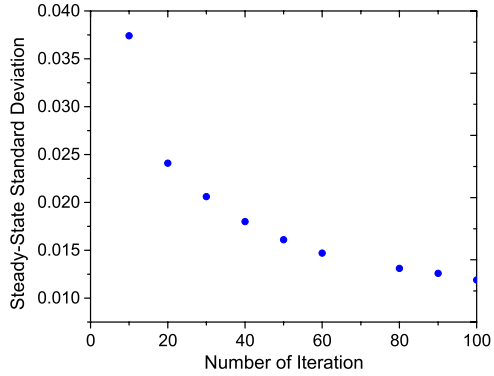

Fig. 5. (Color online) Plot of the system excited-state population variance after reaching the steady state versus the number of simulations for a reservoir dimension of 12. The parameters used in the plot are $\Omega_s = 1$, $E_r = 1$, $E_{sr} = 0.15$, $N = 12$.

over 30 time evolutions, as shown in Fig. 5, the standard deviation of the steady-state value is around 0.022. This translates to a 5% error relative to the steady-state value of 0.5. Additionally, the standard deviation decreases with increasing reservoir dimension N, as seen in Fig. 6, thus allowing fewer simulations to get the same percent error. From the results of Figs. 2 and 6, an increasing reservoir dimension N causes both an increase in decoherence and a decrease in the standard deviation.

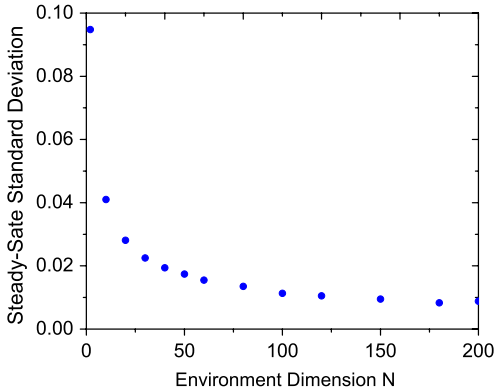

Fig. 6. (Color online) Plot of the system steady-state population variance after averaging 10 runs versus the reservoir dimension N. The mean steady-state value is around 0.5. The parameters used in the plot are $\Omega_s = 1$, $E_r = 1$, $E_{sr} = 0.15$.

4. DISCUSSION AND SUMMARY

Up to this point this article has compared the RMT approach with the standard master equation in the Markovian regime. The RMT was able to model non-Markovian processes. A few other methods used to simulate non-Markovian include variations of unravelling of the stochastic Schrödinger equation. Some of these methods include using doubled or trippled Hilbert space methods [21,22], a non-Markovian quantum state distribution method [14,23], and a non-Markovian quantum jump method [24,25]. Each of these methods adds the memory effect of the non-Markovian process in different ways. However, all of these methods based on stochastic simulations make various approximations that may reduce the ability to use them in general quantum system cases. Another advantage of RMT is that it solves the Schrödinger wave equation without any approximations besides making the reservoir of finite size.

One other method used by Budini involves using random Lindblad operators to model non-Markovian systems [4]. In the paper, the complex reservoir is split into a number of subreservoirs each with a random decay rate in order to observe non-Markovian effects. The ability to simulate the non-Markovian effects comes about in this model because the system evolution depends on the history of which subreservoirs are visited on a particular simulation. From the perspective of describing non-Markovian behavior, both approaches are similar; however, the random matrix model is easier to implement and naturally includes decoherence.

In summary, this article has used RMT to model a quantum system interacting with a reservoir in both the Markovian and non-Markovian regimes. The results from RMT and the master equation agreeing in the Markovian region. The wave function random matrix theory exhibits non-Markovian dynamics when the atomic system is strongly coupled to the reservoir. The decoherence increases with reservoir dimension and decreases with coupling strength. The standard deviation of the population decreases as the reservoir dimension N and number of simulations increase.

ACKNOWLEDGMENTS

The author acknowledges valuable discussions with J. Eberly, H. Batelaan, and A. Marino.

REFERENCES

1. W. H. Zurek, "Decoherence and the transition from quantum to classical," Phys. Today **44**, 36–44 (1991).
2. C. Kiefer, D. J. W. Giulini, J. Kupsch, I.-O. Stamatescu, E. Joos, and H. D. Zeh, *Decoherence and the Appearance of a Classical World in Quantum Theory* (Springer, 2010).
3. G. Lindblad, "On the generators of quantum dynamical semigroups," Commun. Math. Phys. **48**, 119–130 (1976).
4. A. A. Budini, "Random Lindblad equations from complex environments," Phys. Rev. E **72**, 056106 (2005).
5. X. L. Huang, H. Y. Sun, and X. X. Yi, "Non-markovian quantum jump with generalized Lindblad master equation," Phys. Rev. E **78**, 041107 (2008).
6. M. Genkin, E. Waltersson, and E. Lindroth, "Estimation of the spatial decoherence time in circular quantum dots," Phys. Rev. B **79**, 245310 (2009).
7. T. A. Brody, J. Flores, J. B. French, P. A. Mello, A. Pandey, and S. S. M. Wong, "Random-matrix physics: spectrum and strength fluctuations," Rev. Mod. Phys. **53**, 385–479 (1981).
8. J. Gong and P. Brumer, "Coherent control of quantum chaotic diffusion," Phys. Rev. Lett. **86**, 1741–1744 (2001).
9. F. Franchini and V. E. Kravtsov, "Horizon in random matrix theory, the hawking radiation, and flow of cold atoms," Phys. Rev. Lett. **103**, 166401 (2009).
10. C. Pineda, T. Gorin, and T. H. Seligman, "Decoherence of two-qubit systems: a random matrix description," New J. Phys. **9**, 1–35 (2007).
11. M. Sadgrove, S. Wimberger, S. Parkins, and R. Leonhardt, "Scaling law and stability for a noisy quantum system," Phys. Rev. E **78**, 025206 (2008).
12. H. J. Carmichael, *Statistical Methods in Quantum Optics* (Springer, 1996).
13. G. J. Milburn and D. F. Walls, *Quantum Optics* (Springer, 1994).
14. W. T. Strunz, L. Diósi, and N. Gisin, "Open system dynamics with non-Markovian quantum trajectories," Phys. Rev. Lett. **82**, 1801–1805 (1999).
15. J. Piilo, S. Maniscalco, K. Härkönen, and K.-A. Suominen, "Non-Markovian quantum jumps," Phys. Rev. Lett. **100**, 180402 (2008).
16. R. Vasile, S. Olivares, M. A. Paris, and S. Maniscalco, "Continuous-variable quantum key distribution in non-Markovian channels," Phys. Rev. A **83**, 042321 (2011).
17. K.-L. Liu and H.-S. Goan, "Non-Markovian entanglement dynamics of quantum continuous variable systems in thermal environments," Phys. Rev. A **76**, 022312 (2007).
18. B. Misra and E. C. G. Sudarshan, "The zeno's paradox in quantum theory," J. Math. Phys. **18**, 756–763 (1977).
19. F. M. Spedalieri, H. Lee, M. Florescu, K. T. Kapale, U. Yurtsever, and J. P. Dowling, "Exploiting the quantum zeno effect to beat photon loss in linear optical quantum information processors," Opt. Commun. **254**, 374–379 (2005).
20. S. Mancini and R. Bonifacio, "Quantum zeno-like effect due to competing decoherence mechanisms," Phys. Rev. A **64**, 042111 (2001).
21. H.-P. Breuer, B. Kappler, and F. Petruccione, "Stochastic wave-function method for non-Markovian quantum master equations," Phys. Rev. A **59**, 1633–1643 (1999).
22. H.-P. Breuer, "Genuine quantum trajectories for non-Markovian processes," Phys. Rev. A **70**, 012106 (2004).
23. J. T. Stockburger and H. Grabert, "Exact *c*-number representation of non-Markovian quantum dissipation," Phys. Rev. Lett. **88**, 170407 (2002).
24. J. Piilo, S. Maniscalco, K. Härkönen, and K.-A. Suominen, "Non-Markovian quantum jumps," Phys. Rev. Lett. **100**, 180402 (2008).
25. J. Piilo, K. Härkönen, S. Maniscalco, and K.-A. Suominen, "Open system dynamics with non-Markovian quantum jumps," Phys. Rev. A **79**, 062112 (2009).